URSI GASS 2021, Rome, Italy, 28 August - 4 September 2021

Interannual variability of water vapour and tropical tropopause temperature: Zonal structure

KV. Suneeth* (1), and SS. Das (2)
(1) India Meteorological Department (IMD), New Delhi, India
(2) Space Physics Laboratory, Vikram Sarabhai Space Centre, Thiruvananthapuram, Kerala, India

Abstract

We quantified the interannual coupling between temperature and water vapour in the Tropical Tropopause Layer (TTL) using 10 years of satellite based observations. The correlation pattern between deseasonalized anomalies of temperature (in terms of saturation mixing ratio) and water vapour mixing ratio shows a strong zonal structure, with peak correlation values in the TTL (between 15 km and cold-point level) over Maritime Continents including western Pacific Ocean (90°E to 180°E), and Atlantic Ocean (0 to 50°W). The Quasi-Biennial Oscillation amplitude in cold-point temperature (CPT-T) is more or less zonally symmetric, with peak value over the Maritime Continent and Atlantic Ocean. During El-Nino event, CPT-T over the western Pacific and Maritime Continent are largely influenced with warm anomaly. Associate with this CPT-T variation, large enhancement in 100 hPa is noticed over the Indian Ocean between 20°N-S latitude. The difference between zonal mean deseasonalized anomalies of 100 hPa water vapour and saturation mixing ratio at cpt show significant fluctuations (±0.3 ppmv) that are roughly coincide with the Oceanic Nino Index with a 6 month lag.

1 Introduction

Stratospheric water vapour variations are strongly related to tropical cold-point tropopause on different time scales. Eventhough the relation between tropopause temperature and water vapour variabilities on subseasonal to annual scales are known, the interannual variability is least known. The El-Nino Southern Oscillation (ENSO) and Quasi-biennial Oscillation (QBO) are the key modes of interannual temperature variability in the upper troposphere and lower stratosphere (UTLS) region. The phases of ENSO and QBO are critical in determining the longitudinal distribution of water vapour over the tropics [1]. Based on simulations, [2] examined zonally resolved impact of ENSO on stratospheric water vapour entry values. Authors found wet and dry anomalies in the stratospheric water vapour transport during El Nino and La Nina winters respectively. Generally temperature profiles for the tropopause studies are taken from radiosonde sounding with limited spatial and temporal sampling or from reanalysis data with coarse vertical resolution. In most of the previous studies, the relationship between CPT temperature and stratospheric water vapour are discussed mainly focusing on the zonal mean values [3]. But the regional influence of TTL temperature variabilities on local water vapour distribution is not quantified based on long-term independent observations.

Presently, the availability of long-term global data from Constellation Observing System for Meteorology, Ionosphere, and Climate (COSMIC) radio occultation measurements, with relatively high vertical resolution, provides a unique opportunity to quantify the zonal variability in CPT temperature over the tropics. Combined analysis of temperature and water vapour variabilities using measurements of COSMIC and Aura-Microwave Limb Sounder (MLS) respectively, are expected to provide finer details of the coupling of water vapour with TTL temperature. In the present study, we calculate saturation mixing ratio corresponding to the TTL temperature and then compare this calculation with local water vapour measurements in the TTL.

2 Data and methodology

2.1 Water vapour from MLS measurements

Our analysis is based on the water vapour measurements obtained from space-borne MLS onboard the Aura satellite. Detailed description of measurement techniques, resolution, precision, and accuracy of Aura-MLS dataset is provided in [4]. Water vapour profiles are retrieved from 190 GHz radiance measurements. We use the version 4.2 level-2 data. In water vapour profiles, the vertical resolution range is between 1.3 to 3.6 km from 316 to 0.22 hPa, with a horizontal resolution of 170 to 350 km along the track. An accuracy of 8-15% and precision of 15-20% with the minimum of 0.1 ppmv is found in water vapour measurement. Aura-MLS provides about 3500 profiles per day. The analysed monthly mean data are gridded with a resolution of 2.5 degree (latitude) x 5 degree (longitude) for the period 2007 to 2016.

2.2 Temperature from Radio Occultation measurements

The UTLS temperatures for the present study are from the COSMIC radio occultation measurements. A detailed description of retrieval techniques of radio occultation temperature data can be found in [5]. The vertical resolution in the GPS-RO measurements is about 1 km

near the tropopause method. We use moist-air retrieval temperature profiles for the period 2007 to 2016 which are interpolated onto a 100m vertical grid. The temperature measurements have a precision of 0.1% between 8 and 25 km. The temperature accuracy in the UTLS region is 0.5 K for individual profile and 0.1 K for averaged profiles [6]. Globally, the number of COSMIC occultation events per day is about 1500–2000. We use individual COSMIC temperature profiles to determine the cold-point or the temperature minimum. The altitude corresponding to the cold-point tropopause temperature (CPT-T) is taken as the cold-point tropopause altitude (CPT-A). Since the cold-point is not well defined outside the tropics, in the present study we restricted the analysis for 30°N-30°S latitude band.

2.3 QBO and ENSO Indices

In the present study, 50 hPa Singapore zonal wind data is taken as the proxy for Quasi-Biennial Oscillation (QBO) variability The Oceanic Nino Index (ONI) is taken as the 3 month running mean of Sea Surface Temperature anomalies at Nino 3.4 region. Monthly mean deseasonalized CPT-T anomalies at each grid are linearly regressed with respect to normalized QBO and ENSO indices individually to extract the response of such oscillations in CPT-T. We then use this regression coefficient to infer the interannual changes in CPT-T that are linked to QBO and ENSO.

2.4 Estimation of saturation mixing ratio

At the cold point temperatures, we estimated corresponding saturation mixing ratio (SMR_{cpt}) by using equation-7 of [7]. To account for the non-linearity of the Clausius-Clapeyron equation, we estimated the SMR_{cpt} for each CPT-T individually and then averaged to get monthly mean data with a grid resolution of 2.5 degree (latitude) x 5 degree (longitude). We consider MLS water vapour measurement at 100 hPa (WMR_{100}) as equivalent to water vapour measurement at cold-point level; since 100 hPa pressure level being the available nearest level to the climatological CPT altitude. Sample time series showing deseasonalized time series of monthly mean anomalies of estimated SMR_{cpt} and observed WMR_{100} over western Pacific are illustrated in Figure 1. The data are deseasonalized with respect to long-term mean annual cycle at each grid point.

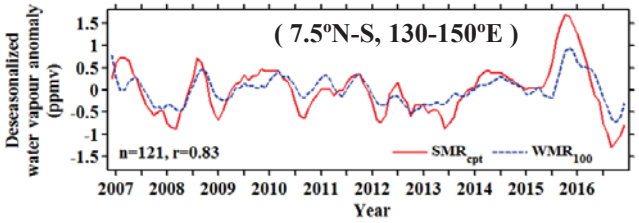

Figure 1. Time series of deseasonalized monthly mean anomalies of saturation mixing ratio at CPT (SMR_{cpt}) and water vapour mixing ratio at 100 hPa (WMR_{100}) over western Pacific.

We also calculated saturation mixing ratios to temperatures at specific altitudes in the UTLS region that are equivalent to MLS pressure levels. We found that even though MLS water vapour retrievals represent layer averages of 2-3 km thick, the annual and interannual anomalies near tropopause are in quantitative agreement with reconstructed saturation mixing ratio from the COSMIC temperature anomalies.

3 Results and discussion

3.1 Interannual variability in SMR-WMR relationship: Horizontal and vertical map

The SMR_{cpt}-WMR_{100} correlation coefficients for the tropics with a 2.5×5 (lat×lon) grid resolutions is shown in Figure 2a. The correlation pattern shows a strong zonal structure, with peak correlation values over the following regions: a) Maritime Continents including western Pacific Ocean (90°E to 180°E), and b) Atlantic Ocean (0 to 50°W). These higher correlation values indicate a strong coupling between interannual variabilities of CPT-T and water vapour over these regions. These regions of highest correlation are found to be different from the estimation of [8], based on the reanalysis dataset.

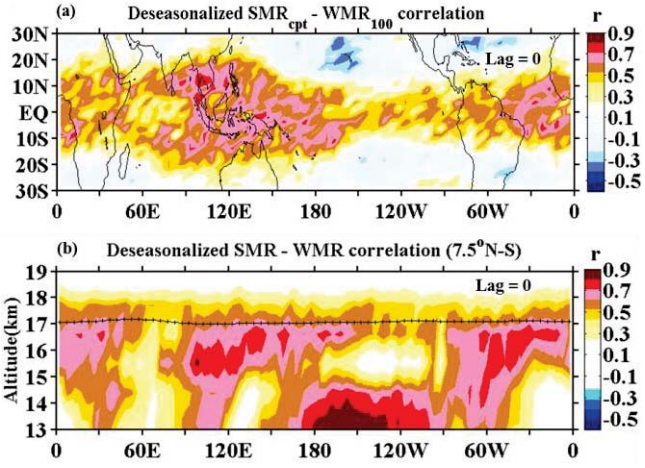

Figure 2. (a) Latitude-longitude structure of correlation coefficients between deseasonalized anomalies of saturation mixing ratio (SMR) at CPT and water vapour mixing ratio at 100 hPa (WMR_{100}). (b) Longitude-altitude structure (7.5°N-S) of correlation coefficients between deseasonalized SMR anomalies at tropical tropopause layer (TTL) temperature and corresponding WMR anomalies at each MLS pressure levels. Both the anomalies are smoothed by 3 month running mean.

Further, we explore the vertical structure of SMR-WMR correlation pattern in the TTL. Here we correlated deseasonalized near-equatorial (7.5°N-S) anomalies of SMR and WMR as a function of pressure level and longitude and shown in Figure 2b. The regions with highest correlations in Figure 2b are consistent with the observed horizontal picture in Figure 2a. In the TTL, highest interannual correlation coefficients are noticed

between 15 km and CPT-A over a) Maritime continent including western Pacific and b) Atlantic Ocean. It is interesting to note the westward tilt of peak correlation values at the Atlantic region. In the upper troposphere, below ~14 km strong correlations over Nino source region are due to the connection between El Nino related tropospheric warming and enhanced convention that leads to more water vapour in the upper troposphere. The interannual variabilities of temperature and water vapour in the TTL are attributed to the QBO and ENSO modes.

3.2 Separation of QBO / ENSO components

To estimate the influence of QBO and ENSO on the CPT-T variability, a linear regression analysis is performed individually between interannual anomalies of CPT-T and indices of QBO or ENSO. Cross correlation analysis between QBO index (50 hPa zonal wind) and CPT-T indicated a phase shift of 2 months between two parameters. Regression coefficients are estimated considering this 2 month phase shift between CPT temperature and QBO index. Figure 3a represents the QBO regression coefficient of CPT-T.

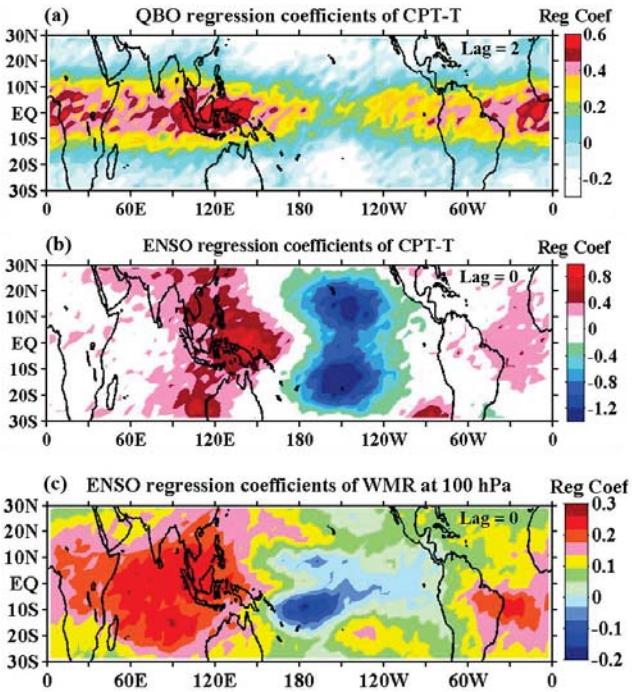

Figure 3. Univariate linear regression coefficients of CPT-T with (a) QBO and (b) ENSO indices. (c) Univariate linear regression coefficients of WMR_{100} with ENSO index. The QBO and ENSO indices are 50 hPa Singapore zonal wind and Sea Surface Temperature anomalies at Nino 3.4 region respectively.

The QBO regression map shows an equatorial maximum that reduces with increase in latitude and extends up to 10°N-S. The QBO amplitude in CPT-T is more or less zonally symmetric, with peak influence of QBO on CPT-T over the Maritime Continent and Atlantic Ocean near east Africa, and with less influence over the Nino region in the central Pacific. Similarly, the ENSO influence on the CPT-T is represented by the ENSO regression coefficients of CPT-T in Figure 3b. The dumbbell pattern, a characteristic ENSO pattern, in the off-equatorial region of central Pacific, is clear in the regression map and is attributed to the Rossby and Kelvin wave circulations induced by equatorial heating [9, 10]. The regression map indicate that, during El Nino period, CPT-T over the western Pacific and Maritime Continent are largely influenced with warm anomaly, while off-equatorial region in the central Pacific with cold anomaly. Unlike QBO component, the ENSO related component in the Pacific Ocean produce a zonally asymmetric changes in the CPT-T. To examine how these zonally asymmetric changes in the CPT-T reflect in 100hPa water vapour, we performed a linear regression analysis between 100 hPa water vapour anomaly and ENSO index. The resulting ENSO regression coefficient map of WMR_{100} is shown in Figure 3c. A large enhancement in WMR100 is noticed over the Indian Ocean between 20°N-S latitude and relatively small enhancement over the western side of Atlantic Ocean near ~10°S. The dumbbell pattern is also visible near the date line with cold anomaly.

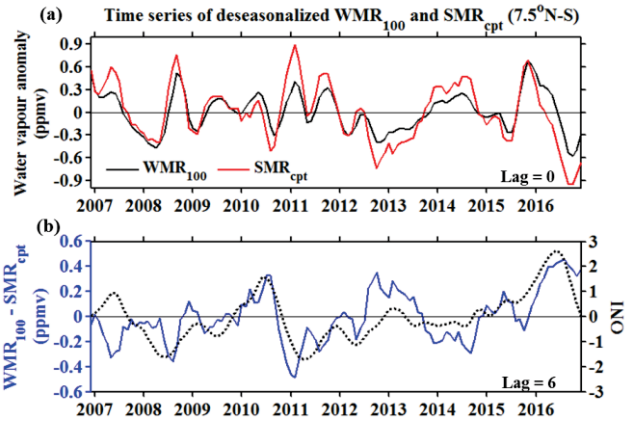

Figure 4. (a) Monthly mean deseasonalized anomalies of saturation mixing ratio at cold- point (red line) and water vapour mixing ratio at 100 hPa (black line) averaged over near-equatorial region. (b) Difference between above mentioned anomalies, indicated by blue curve. The dotted black line indicates the Oceanic Nino Index (ONI) (lagged by six months).

The interannual anomalies of water vapour entry mixing ratio are dominated by anomalies of zonal mean temperature [11]. In order to estimate the influence of zonally asymmetric ENSO component in zonal mean values of CPT-T and thus to examine the how well the zonal mean SMR_{cpt} represent the zonal mean WMR_{cpt}, we plotted the time series of near-equatorial (7.5°N-S) zonal mean SMR_{cpt} and WMR_{100} in Figure 4a and their differences in 4b. The zonal mean values of estimated and observed water vapour are in good agreement. The difference between the anomalies (blue line in Figure 4b) show significant fluctuations (±0.3 ppmv) that are roughly coincide with the Oceanic Nino Index (ONI, shown by dotted black line, and is shifted by 6 months to maximize

the correlation). El Nino events largely influence the normal Walker circulation by shifting the region of deep convection eastward towards the central Pacific [10]. Previous studies reported that ENSO related atmospheric temperature anomalies show two components in the equatorial region: a zonal mean component and eddy component [12]. While atmospheric eddy component responds rapidly to ENSO forcing (~1 month), zonal mean component responds with a lag of ~3 months to the SST anomalies in the eastern equatorial Pacific. In Figure 4, a lag of ~ 6 months in the difference in anomalies attributed to the contribution of zonal mean component.

4 Summary and concluding remarks

Strong convection over the tropics largely influences the transport of water vapour into the TTL. In the TTL, above ~15 km, dynamically driven large-scale upwelling drives a significant annual cycle in temperature. These temperature variations control the water vapour present in the air during its slow ascent to the stratosphere. In the present study, we aim to quantify the interannual coupling between tropopause temperature and water vapour over the tropics. We correlated interannual anomalies of the estimated saturation mixing ratio (SMR) from TTL temperature with observed water vapour mixing ratio (WMR) during the period 2007-2016. From the study following salient features are brought out,

a) The interannual correlation pattern shows a strong zonal structure, with peak correlation values over the following regions: a) Maritime Continents including western Pacific Ocean (90°E to 180°E), and b) Atlantic Ocean (0 to 50°W).

b) In the TTL, highest correlation coefficients for SMR-WMR deseasonalized anomalies are noticed between 15 km and CPT-A over 1) Maritime continent including western Pacific and 2) Atlantic Ocean.

c) The QBO amplitude in CPT-T is more or less zonally symmetric, with peak influence over the Maritime Continent and Atlantic Ocean near east Africa, and with less influence over the Nino region in the central Pacific.

d) During ENSO event, CPT-T over the western Pacific and Maritime Continent is largely influenced with warm anomaly, while off-equatorial region in the central Pacific with cold anomaly. Associate with this CPT-T variation, large enhancement in WMR_{100} is noticed over the Indian Ocean between 20°N-S latitude.

e) The difference between interannual anomalies of WMR_{100} and SMR_{cpt} show significant fluctuations (±0.3 ppmv) that are roughly coincide with the Oceanic Nino Index lagged by 6 months.

5 Acknowledgements

Authors would like to acknowledge Goddard Earth Sciences Data and Information Services Centre and UCAR/CDAAC team for providing the Aura-MLS and COSMIC data. One of the author, KVS thankful to Indian Space Research Organization (ISRO) for providing doctoral fellowship during this study period.

6 References

1. C.K. Liang, A. Eldering, A. Gettelman et al, "Record of tropical interannual variability of temperature and water vapor from a combined AIRS-MLS data set," *Journal of Geophysical Research: Atmospheres,* 116, D6, March 2011, doi: 10.1029/2010JD014841.

2. P. Konopka, F. Ploeger, M.Tao, and M. Riese, "Zonally resolved impact of ENSO on the stratospheric circulation and water vapor entry values," *Journal of Geophysical Research: Atmospheres,* 121, 19, October 2016, pp. 11-486, doi: 10.1002/2015JD024698.

3. M. Diallo, M. Riese, T. Birner et al, "Response of stratospheric water vapor and ozone to the unusual timing of El Niño and the QBO disruption in 2015–2016," *Atmospheric Chemistry and Physics,* 18, 17, September 2018, pp. 13055-13073, doi: 10.5194/acp-2018-239.

4. N. J. Livesey, W. G. Read, P. A. Wagner et al, "EOS MLS Version 4.2 x Level 2 data quality and description document," *Jet Propulsion Laboratory, California Institute of Technology, Pasadena, CA* (2015).

5. E. R. Kursinski, G. A. Hajj, J. T. Schofield et al, "Observing Earth's atmosphere with radio occultation measurements using the Global Positioning System," *Journal of Geophysical Research: Atmosphere,* 102, D19, October 1997, pp. 23429-23465, doi:10.1029/97JD01569.

6. G. A. Hajj, C. O. Ao, B. A. Iijima, and D. Kuang "CHAMP and SAC-C atmospheric occultation results and intercomparisons," *Journal of Geophysical Research: Atmospheres,* 109, D6 March 2004, doi: 10.1029/2003JD003909.

7. D. M. Murphy, and T. Koop, "Review of the vapour pressures of ice and supercooled water for atmospheric applications," *Quarterly Journal of the Royal Meteorological Society,* 131, 608, April 2005, pp. 1539-1565, doi: 10.1256/qj.04.94.

8. W. J. Randel, F. Wu, S. J. Oltmans et al, "Interannual changes of stratospheric water vapor and correlations with tropical tropopause temperatures," *Journal of the Atmospheric Sciences,* 61, 17, September 2004, pp. 2133-2148, doi:10.1175/1520-0469(2004)061<2133:ICOSWV>2.0.CO;2.

9. A. E. Gill, "Some simple solutions for heat-induced tropical circulation," *Quarterly Journal of the Royal Meteorological Society,* 106, 449, July 1980, pp. 447-462, doi:10.1002/qj.49710644905.

10. E. Yulaeva, and J. M. Wallace, "The signature of ENSO in global temperature and precipitation fields derived from the microwave sounding unit," *Journal of climate,* 7, 11, November 1994, pp. 1719-1736, doi:10.1175/1520-0442(1994)007<1719:TSOEIG>2.0.CO;2

11. S. Fueglistaler, P. H. Haynes, and E. Nin, "Control of interannual and longer-term variability of stratospheric water vapor," *Journal of Geophysical Research: Atmospheres,* 110, D24, December 2005, doi: 10.1029/2005JD006019

12. B. Scherllin-Pirscher, C. Deser, S. P. Ho, C. Chou, W. Randel, and Y. H. Kuo, "The vertical and spatial structure of ENSO in the upper troposphere and lower stratosphere from GPS radio occultation measurements," *Geophysical Research Letters,* 39, 20, October 2012, doi: 10.1029/2012GL053071.